Stem Cell Reports
Article

OPEN ACCESS

Transcriptionally and Functionally Distinct Mesenchymal Subpopulations Are Generated from Human Pluripotent Stem Cells

Chee Jia Chin,[1] Suwen Li,[1] Mirko Corselli,[2] David Casero,[1] Yuhua Zhu,[1] Chong Bin He,[1] Reef Hardy,[3,4,5,6] Bruno Péault,[1,3,4,5,7] and Gay M. Crooks[1,5,8,9,*]

[1]Department of Pathology and Laboratory Medicine, David Geffen School of Medicine (DGSOM), University of California (UCLA), Los Angeles, CA 90095, USA
[2]Becton Dickinson, San Diego, CA 92121, USA
[3]Department of Orthopedics, DGSOM, UCLA, Los Angeles, CA 90095, USA
[4]Orthopedic Hospital Research Center, UCLA, Los Angeles, CA 90095, USA
[5]Broad Stem Cell Research Center (BSCRC), UCLA, Los Angeles, CA 90095, USA
[6]Department of Medicine, University of Indiana, Indianapolis, IN 46202, USA
[7]Center for Regenerative Medicine, University of Edinburgh, Edinburgh EH16 4UU, UK
[8]Department of Pediatrics, DGSOM, UCLA, Los Angeles, CA 90095, USA
[9]Jonsson Comprehensive Cancer Center (JCCC), UCLA, Los Angeles, CA 90095, USA
*Correspondence: gcrooks@mednet.ucla.edu
https://doi.org/10.1016/j.stemcr.2017.12.005

SUMMARY

Various mesenchymal cell types have been identified as critical components of the hematopoietic stem/progenitor cell (HSPC) niche. Although several groups have described the generation of mesenchyme from human pluripotent stem cells (hPSCs), the capacity of such cells to support hematopoiesis has not been reported. Here, we demonstrate that distinct mesenchymal subpopulations co-emerge from mesoderm during hPSC differentiation. Despite co-expression of common mesenchymal markers (CD73, CD105, CD90, and PDGFRβ), a subset of cells defined as $CD146^{hi}CD73^{hi}$ expressed genes associated with the HSPC niche and supported the maintenance of functional HSPCs *ex vivo,* while $CD146^{lo}CD73^{lo}$ cells supported differentiation. Stromal support of HSPCs was contact dependent and mediated in part through high *JAG1* expression and low WNT signaling. Molecular profiling revealed significant transcriptional similarity between hPSC-derived $CD146^{++}$ and primary human $CD146^{++}$ perivascular cells. The derivation of functionally diverse types of mesenchyme from hPSCs opens potential avenues to model the HSPC niche and develop PSC-based therapies.

INTRODUCTION

Maintenance of *bona fide* self-renewing hematopoietic stem and progenitor cells (HSPCs) *ex vivo* remains challenging in part because of our limited ability to recapitulate the human HSPC niche in culture. Intensive research efforts have begun to uncover the cellular and molecular constituents of the niche that regulate self-renewal and differentiation of HSPCs. Through the use of knockout and transgenic mice, several cell populations have been described in terms of their spatial relationship to the bone and blood vessels of the bone marrow, and their differential expression of various markers and bioactive molecules (Ding et al., 2012; Itkin et al., 2016; Kobayashi et al., 2010; Kunisaki et al., 2013).

High expression of melanoma-associated cell adhesion molecule (CD146) identifies human pericytes, a cell type that ensheaths capillaries, venules, arterioles, and sinusoids (Crisan et al., 2008) and can establish a heterotopic hematopoietic stem cell (HSC) niche when transplanted into immunodeficient mice (Sacchetti et al., 2007). Unlike $CD146^{-}$ mesenchyme, monolayers of $CD146^{++}$ cells isolated from primary tissue (adult adipose tissue and fetal bone marrow) can support human HSPCs co-cultured for at least 2 weeks in the absence of exogenous cytokines (Corselli et al., 2013).

We and others have shown that mesenchymal cells can be differentiated from human pluripotent stem cells (hPSCs) (Chin et al., 2016; Ferrell et al., 2014; Hoffman and Calvi, 2014; Vodyanik et al., 2010). These previous studies identified mesenchyme as a single population defined mostly by expression of CD73 and/or CD105 and absence of hematopoietic and endothelial markers. We now report that the mesenchyme generated from hPSCs is functionally and transcriptionally heterogeneous. Our studies identified a distinct subpopulation of hPSC-derived mesenchyme that expressed high levels of CD146 and CD73 and low levels of PDGFRα (CD140a) and that was capable of supporting clonogenic, engraftable, and self-renewing human HSPCs *ex vivo* without exogenous cytokines. In contrast $CD146^{lo}CD73^{lo}$ mesenchyme showed significantly less capacity to support HSPCs. Transcriptome analysis revealed that the $CD146^{hi}CD73^{hi}$ cells expressed significantly higher levels than $CD146^{lo}CD73^{lo}$ cells of perivascular markers and niche factors known to have critical roles in HSC maintenance. HSPC support was dependent in part on cell-cell interactions and Notch signaling through stromal expression of JAG1, whereas

differentiation was promoted by WNT signaling. Closer transcriptional analysis, combining data from mesenchyme generated from hPSCs and human primary tissue, revealed that dominant pathways shared by the CD146^{++} populations were those related to vascular development, cell adhesion, and motility. Our data suggest that hPSC-derived mesoderm can generate mesenchymal cells phenotypically, functionally, and molecularly, similar to previously identified primary pericytes that contribute to the human HSPC niche.

RESULTS

Heterogeneity of Embryonic Mesoderm-Derived Mesenchymal Cells

We have previously characterized a human embryonic mesoderm progenitor (hEMP) population derived from hPSCs that marks the onset of mesoderm commitment and has the potential to generate a broad range of mesodermal derivatives, including mesenchyme, endothelium, and bone, three lineages that play a crucial role in the hematopoietic niche (Chin et al., 2016; Hoffman and Calvi, 2014). hEMPs were isolated at day 3.5 of mesoderm differentiation from H1 embryonic stem cells (Evseenko et al., 2010) (Figure 1A), and re-cultured using conditions that favor mesenchymal differentiation. After a further 14 days, cultures contained a mixture of CD31^{+}CD45^{-} endothelial cells and CD31^{-}CD45^{-} mesenchymal cells. The mesenchymal cells consisted of at least two populations that could be discriminated based on expression of CD146, CD73, and CD140a (PDGFRα) (Figure 1A). High co-expression of CD146 and CD73 identified a largely CD140a^{-} population, whereas CD146^{lo} cells expressed intermediate levels of CD73 and high levels of CD140a. This inverse expression pattern between CD146 and CD140a was consistent with mesenchyme derived from primary human lipoaspirates (Figure S1A). Despite the differential expression of CD146, CD73, and CD140a, both hPSC-derived mesenchymal subsets expressed classic mesenchymal markers CD90, CD105, CD44, and PDGFRβ (Figure S1B). Mesenchymal differentiation from two other hPSC lines, UCLA3 and UCLA6, yielded similar populations to the H1 line, with an inverse relationship of CD146 and CD73 to CD140a expression (Figures S2A and S2B). Although few CD146^{hi}CD73^{hi} cells were present early in differentiation (days 4–5), the inverse expression pattern of CD146 and CD73 to CD140a was present throughout mesenchymal differentiation (Figure S2C).

To better understand whether the phenotypes above identified distinct mesenchymal cell types, we focused our studies on cells that represented the extremes of these phenotypes: a CD146^{hi}CD73^{hi} population and a CD146^{lo}CD73^{lo} population (Figure 1A). Bromodeoxyuridine pulsing of hEMP-derived mesenchymal cultures showed that a significantly higher frequency of CD146^{hi}CD73^{hi} cells were cycling relative to CD146^{lo}CD73^{lo} cells (Figure 1B) ($p \leq 0.05$).

RNA sequencing (RNA-seq) profiling of the two mesenchymal populations demonstrated that 916 genes were differentially expressed (558 up- and 358 downregulated in CD146^{hi}CD73^{hi} relative to CD146^{lo}CD73^{lo} cells; false discovery rate [FDR] < 0.01) (Figure 1C). Across all hESC lines tested, CD146^{hi}CD73^{hi} mesenchyme expressed significantly higher levels of pericyte markers *CSPG4* (which encodes NG2), *NES* (NESTIN), *LEPR* (leptin receptor), and the β2-adrenergic receptor *ADRB2* (Crisan et al., 2008; Hoffman and Calvi, 2014; Kunisaki et al., 2013), and HSC regulatory genes, *KITLG*, *IGFBP2*, and *TNC* (Ding et al., 2012; Huynh et al., 2008; Nakamura-Ishizu et al., 2012; Zhang et al., 2008) (Figures 1C, S1C, S2A, and S2B). In contrast, the CD146^{lo}CD73^{lo} mesenchyme expressed significantly higher levels of the niche factors *CXCL12* and *ADRB3* (Greenbaum et al., 2013; Méndez-Ferrer et al., 2008) (Figure 1C). Expression of extracellular matrix genes was upregulated after the hEMP stage in both mesenchymal phenotypes (Figure 1C).

Mesenchymal Support of HSPCs *Ex Vivo*

The ability of hEMP-derived CD146^{hi}CD73^{hi} and CD146^{lo}CD73^{lo} cells to support HSPCs *ex vivo* was assessed by co-culturing cord blood (CB)-derived CD34^{+} cells on monolayers generated from each mesenchymal population. To determine the specific effect of each stromal subset, cultures were performed in basal medium with a low concentration of serum (5%) and without addition of cytokines.

Although total hematopoietic (CD45^{+} cells) output was similar with both mesenchymal populations (Figure 2A), co-cultures with CD146^{hi}CD73^{hi} cells retained a significantly higher frequency and number of total CD34^{+} cells than co-culture with CD146^{lo}CD73^{lo} mesenchymal cells (Figures 2B and 2C) ($p < 0.01$ and $p < 0.001$, respectively, $n = 16$). In particular, support of the more primitive CD34^{+}Lin^{-} subset was consistently seen in the CD146^{hi}CD73^{hi} co-cultures (Figure 2D). Myeloid output was higher in CD146^{hi}CD73^{hi} co-cultures, whereas more B lymphoid cells were generated on CD146^{lo}CD73^{lo} mesenchyme (Figures 2E and 2F). Significantly more clonogenic cells (colony-forming unit [CFU]-C) were maintained in CD146^{hi}CD73^{hi} co-cultures than CD146^{lo}CD73^{lo} co-cultures ($p < 0.001$, $n = 16$; Figure 2G). Of note, multiple other hPSC-derived phenotypic subsets were screened based on their CD146 and CD140a expression; irrespective

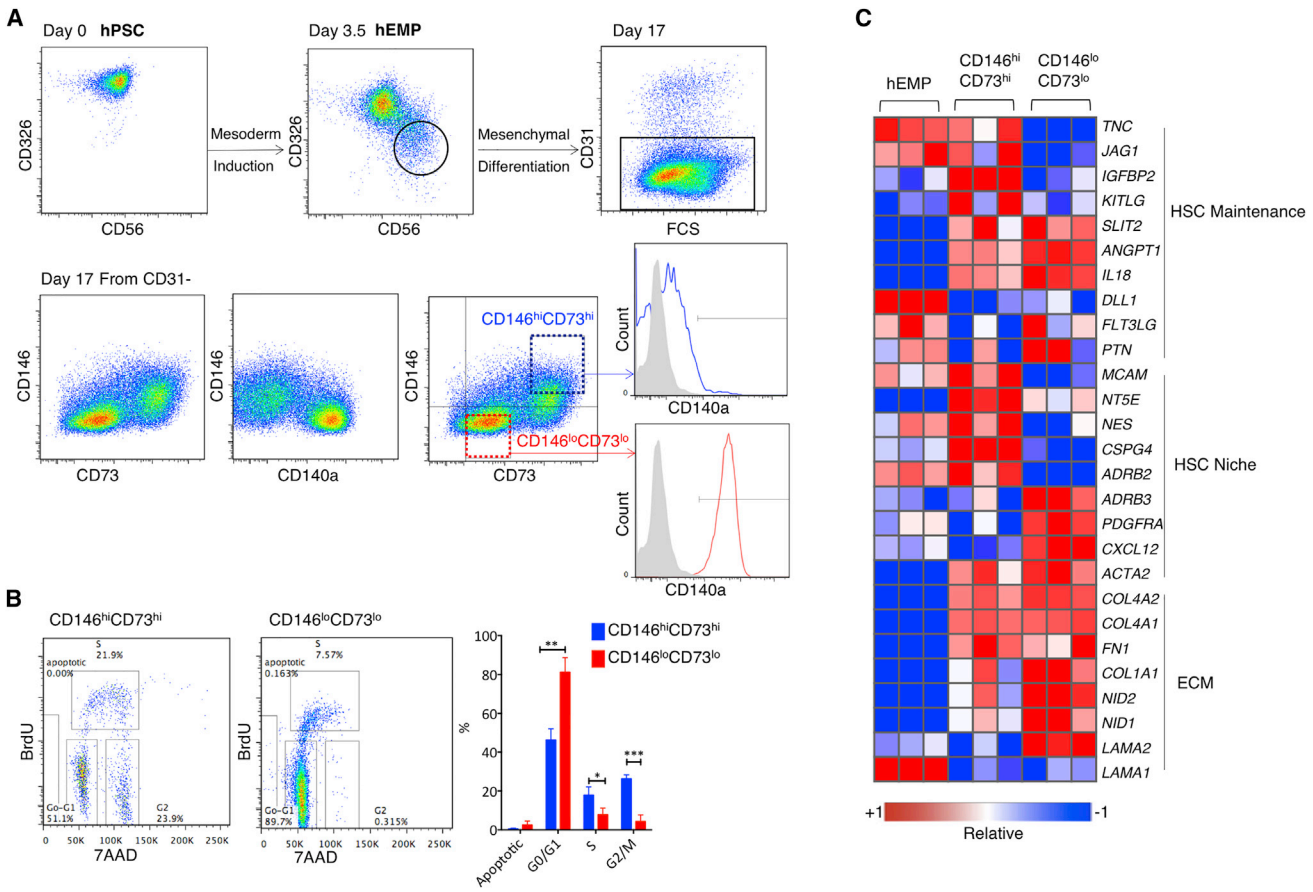

Figure 1. Immunophenotypic Fractionation of hPSC-Derived Mesenchyme Reveals Transcriptionally Distinct Populations

(A) hEMPs were generated from hPSC and isolated at day 3.5 by FACS for further differentiation in mesenchymal conditions. After 2 weeks, two distinct populations were identified within the CD31$^-$ (non-endothelial) cells, which were also CD45$^-$ (non-hematopoietic, not shown). CD146^{lo}CD73^{lo} cells (red) were CD140a$^+$, and CD146^{hi}CD73^{hi} cells (blue) were CD140^{lo} or CD140a$^-$ (representative data using H1 cells of n = 16 experiments).

(B) Cell-cycle analysis of hEMP-derived mesenchymal differentiation cultures at week 2, pulsed with bromodeoxyuridine (BrdU) for 40 min, and gated on CD31$^-$ mesenchyme, as shown in Figure 1A, as either "CD146^{hi}CD73^{hi}" or "CD146^{lo}CD73^{lo}." n = 3 biological replicates. The y axis shows the percentage of each mesenchymal phenotype in each stage of cell cycle, *p < 0.05, **p < 0.01, ***p < 0.001.

(C) Selected genes from RNA-seq profiling of hEMP, and hEMP-derived CD146^{hi}CD73^{hi} and CD146^{lo}CD73^{lo} mesenchyme (as in Figure 1A). Relative expression shown for each gene using its min/max moderate expression estimates as reference. n = 3 biological replicates. Error bars represent SEM. See also Figures S1 and S2.

of CD140a expression, those subsets with high levels of CD146 best supported HSPCs (Figure S3A).

When Lin$^-$CD34$^+$ CD38$^-$ cells, a more primitive HSC-enriched population were studied, the co-culture system was modified by adding exogenous growth factors to allow sufficient cell growth for analysis. In the presence of cytokines, both mesenchymal populations were able to support CD34$^+$ cells for 2–4 weeks. However, only the CD146^{hi}CD73^{hi} mesenchyme could maintain CD34$^+$CD38$^-$CD90$^+$CD45RA$^-$, phenotypic long-term HSCs (n = 4, p < 0.05), and CD34$^+$CD33$^-$ cells (Figure S3B), demonstrating again the functional differences between the two mesenchymal populations in HSPC support.

CD146^{hi}CD73^{hi} Mesenchyme Maintains Human HSPCs with Repopulating Ability and Self-Renewal Potential

To understand whether support of engraftable HSPCs was influenced by the different mesenchymal subsets, equal numbers of CD34$^+$ cells were co-cultured for 2 weeks with CD146^{hi}CD73^{hi} or CD146^{lo}CD73^{lo} cells, and then equal numbers of total hematopoietic cells from the co-cultures were transplanted into sublethally irradiated NOD/SCID/IL-2 receptor$\gamma^{-/-}$ (NSG) mice. Of note, the co-culture conditions were not designed to expand the number of CD34$^+$ cells, as the cultures did not include growth factors (in contrast to all current *ex vivo* expansion protocols).

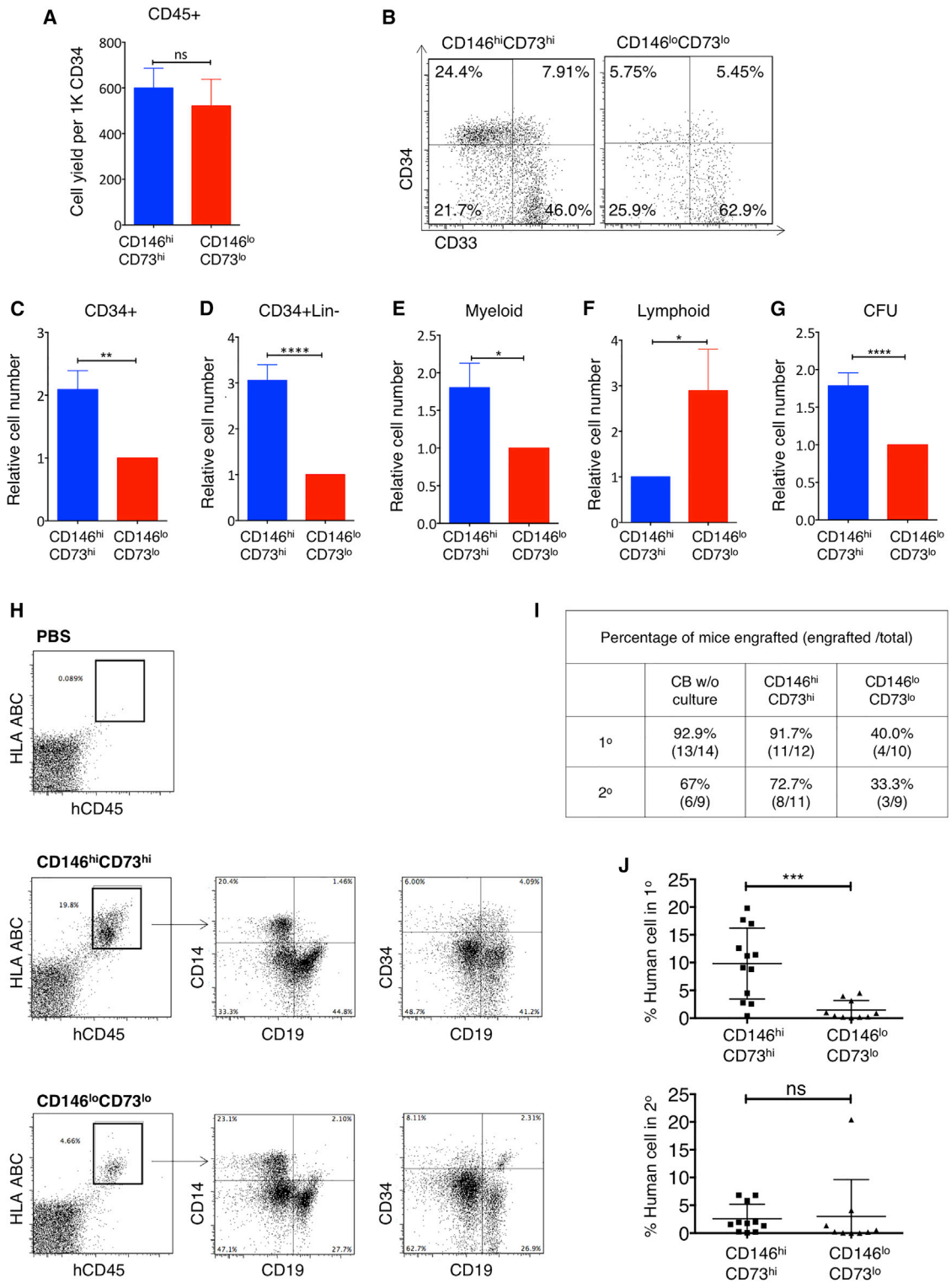

Figure 2. CD146^{hi}CD73^{hi} Mesenchyme Supports *Ex Vivo* Maintenance of Clonogenic, Engraftable, and Self-Renewing HSPCs

CD146^{hi}CD73^{hi} and CD146^{lo}CD73^{lo} mesenchymal cells generated from H1-derived hEMP were isolated and co-cultured as monolayers with CB CD34^{+} cells in 5% serum without added cytokines. After 2 weeks, hematopoietic cells were assayed (A–G) *in vitro* and (H–J) *in vivo*. (A) Total number of live (DAPI^{-}) CD45^{+} cells recovered from co-cultures, shown as cell yield normalized to 1,000 input CD34^{+} cells.

(legend continued on next page)

Based on flow cytometry analysis of bone marrow (Figure 2H), a similar frequency of mice transplanted with hematopoietic cells co-cultured with CD146^{hi}CD73^{hi} cells engrafted (albeit at lower levels) compared with those transplanted with fresh (non-cultured) CD34^{+} cells (11/12 versus 13/14, respectively) (Figures 2I and S3C), whereas only 40% of mice transplanted with hematopoietic cells from CD146^{lo}CD73^{lo} co-cultures demonstrated any detectable engraftment ($\geq$1% huCD45^{+}HLA^{+} cells in bone marrow) ($p < 0.01$) (Figure 2I). CD34^{+} progenitors and multi-lineage reconstitution (CD19^{+} lymphoid cells and CD14^{+} myeloid cells) were detected in the bone marrow, spleen, and peripheral blood of all mice that received hematopoietic cells from CD146^{hi}CD73^{hi} co-cultures (Figure 2H). Levels of engraftment were also significantly higher in animals that received CD146^{hi}CD73^{hi} co-cultures compared with CD146^{lo}CD73^{lo} co-cultures ($p < 0.001$) (Figure 2J). Irrespective of stromal co-culture conditions, mice that demonstrated primary engraftment could engraft in secondary recipients (Figure 2J).

Together, these data indicate that at least two functionally distinct mesenchymal populations were generated from hPSC-derived mesoderm; high CD146 and CD73 expression marked a mesenchymal subpopulation capable of maintaining engraftable HSPCs *ex vivo*, while CD146^{lo}CD73^{lo} mesenchyme had significantly less HSPC-supportive capacity.

HSPC Support Is Sustained through Intercellular Interactions, in Part by Notch Signaling

Prevention of direct contact between CD146^{hi}CD73^{hi} cells and CB CD34^{+} cells using a transwell culture system significantly reduced the number of CD34^{+}Lin^{-} cells maintained in culture ($p < 0.05$, $n = 3$) (Figure 3A). Output of CD146^{lo}CD73^{lo} co-cultures was also reduced in transwells, although to a lesser degree. Thus intercellular mechanisms provide at least part of the HSPC-supportive capacity of CD146^{hi}CD73^{hi} mesenchyme.

Notch signaling is a well-established cell contact-dependent paracrine factor and deletion of Jagged1 (encoded by *Jag1*) results in premature exhaustion of the murine HSC pool (Poulos et al., 2013). Both mesenchymal subsets expressed the Notch ligand *JAG1*, with significantly higher levels in CD146^{hi}CD73^{hi} mesenchyme (Figures 3B, S2A, and S2B); *DLL4* and *DLL1* were not expressed in either mesenchymal population (not shown). Expression of the Notch target *HES1* tended to be higher in the CD34^{+} cells co-cultured with CD146^{hi}CD73^{hi} mesenchyme compared with CD146^{lo}CD73^{lo} supported hematopoietic cells ($p = 0.1789$) (Figure 3C). Addition of a neutralizing antibody to human JAG1 caused a profound (>300-fold) decrease in the number of CD34^{+}Lin^{-} cells in CD146^{hi}CD73^{hi} co-cultures ($p \leq 0.05$, $n = 3$) and 250-fold decrease in CD146^{lo}CD73^{lo} co-cultures (Figure 3D). Of note, cell output was not significantly reduced when anti-JAG1 was added to co-cultures on OP9, a mouse stromal cell line, thus excluding non-specific cytotoxicity from the blocking antibody (Figure S4A).

Thus, although expression of JAG1 was significantly higher in CD146^{hi}CD73^{hi} stroma, HSPC support was dependent on JAG1-mediated activation of Notch signaling in both types of hPSC-mesenchymal co-cultures.

Wnt Inhibitors Are Highly Expressed in CD146^{hi}CD73^{hi} Stroma

Across the entire RNA-seq dataset, the most highly differentially expressed gene between CD146^{hi}CD73^{hi} and CD146^{lo}CD73^{lo} cells was the Wnt antagonist Secreted Frizzled-Related Protein 1 (*SFRP1*) (33-fold difference, FDR < 0.01) (Figure 3E). Expression of other Wnt inhibitors was also significantly higher in CD146^{hi}CD73^{hi} mesenchyme including *SFRP2* (FDR < 0.001) and *DKK1* (FDR < 0.001) (Figure 3E). Expression of Wnt downstream targets *TCF7* and *LEF1* was significantly higher in hematopoietic cells supported by CD146^{lo}CD73^{lo} co-cultures compared with those by CD146^{hi}CD73^{hi} mesenchyme ($n = 5$, $p < 0.05$) (Figure 3F).

Although neither addition of soluble SFRP1 or inhibition of SFRP1 had any detectable effect on HSPCs in either CD146^{hi}CD73^{hi} or CD146^{lo}CD73^{lo} co-cultures (Figure S4B), addition of a Wnt agonist, the GSK-3 inhibitor CHIR99021

(B) Representative FACS analysis of CD45^{+} gated cells from co-cultures.
(C–G) Cell yield of CD34^{+}, CD34^{+} Lin^{-}, CD14^{+} myeloid, CD10^{+}/CD19^{+} B lymphoid cells, and CFU (after re-plating) recovered from 2-week CD146^{hi}CD73^{hi} co-cultures, normalized to CD146^{lo}CD73^{lo} co-cultures.
(A and C–G) n = 16 independent experiments, each in duplicate. Shown are mean ± SEM. *p < 0.05, **p < 0.01, ****p < 0.0001; unpaired two-tailed Student's t test.
(H) Flow cytometry showing gating for the detection of human cells (hCD45^{+}HLA ABC^{+}) and multi-lineage reconstitution after primary transplant. PBS control with no cells injected.
(I) Proportion of mice with engraftment, i.e., detection of >1% human cells after primary transplant (1°) with 1 × 10^{5} CD45^{+} cells obtained either from fresh CB CD34^{+} cells (CB w/o culture), or 2 weeks after co-culture on CD146^{hi}CD73^{hi} or CD146^{lo}CD73^{lo}.
(J) Engraftment (percent of human cells) of mice 6 weeks after primary and secondary transplants (n = 5 independent experiments, total 9–14 mice per group; ***p <.0001; ns, not significant).
Error bars represent SEM. See also Figure S3.

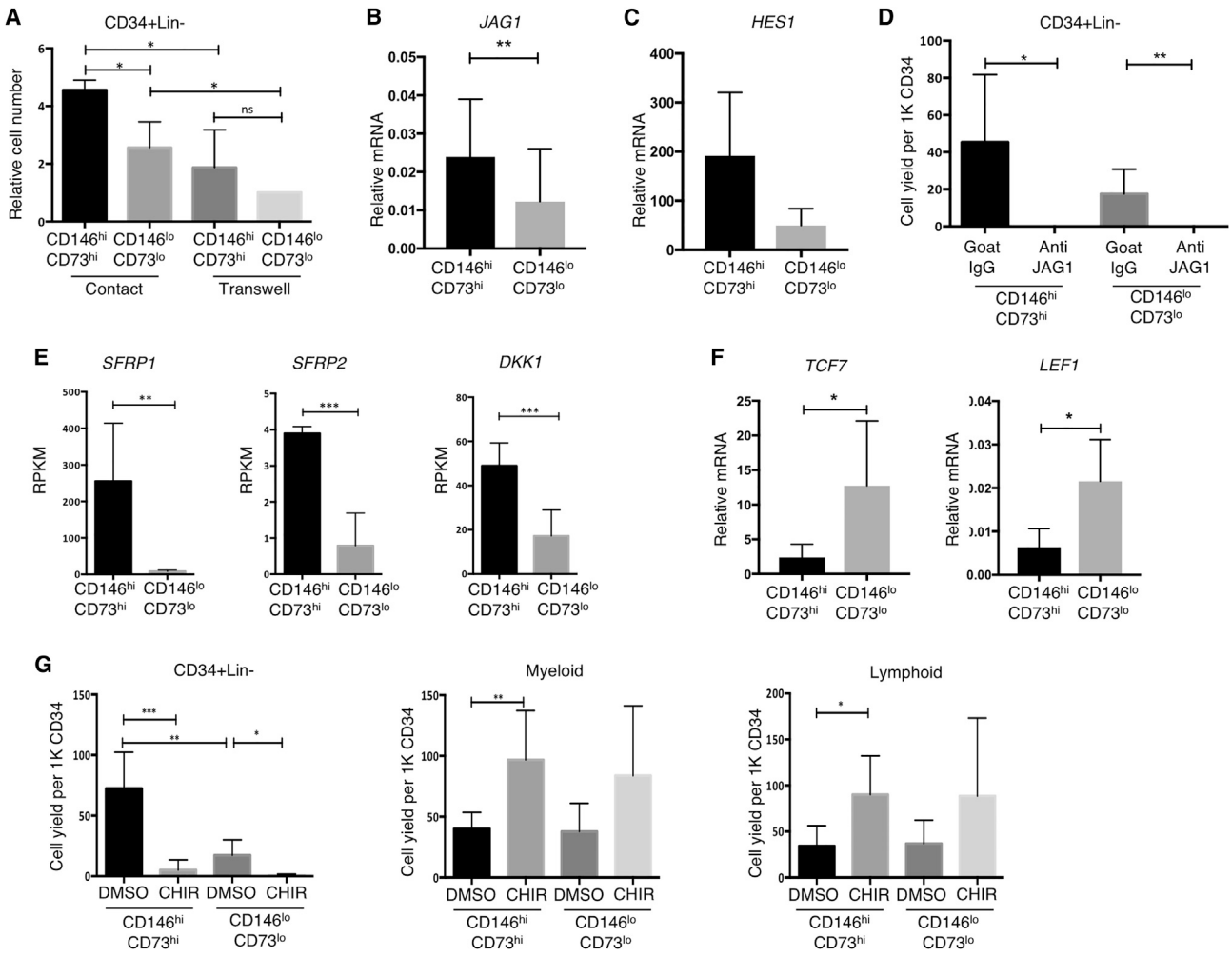

Figure 3. Notch Inhibition and Activation of Wnt Signaling in hPSC-Mesenchyme Co-cultures Leads to Loss of HSPC

(A) Shown is relative number of $CD34^{+}Lin^{-}$ cells in contact and transwell co-culture normalized to yield from $CD146^{lo}CD73^{lo}$ transwell co-cultures (n = 3 independent experiments, mean ± SEM. *p < 0.05).

(B) qRT-PCR of *JAG1* in $CD146^{hi}CD73^{hi}$ and $CD146^{lo}CD73^{lo}$ mesenchyme (n = 14 biological replicates, **p < 0.01).

(C) qRT-PCR of *HES1* in $CD34^{+}$ cells recovered from $CD146^{hi}CD73^{hi}$ and $CD146^{lo}CD73^{lo}$ mesenchyme after 7 days of co-culture without extra cytokines (n = 5 biological replicates, p = 0.1789).

(D) Number of $CD34^{+}$ Lin^{-} cells harvested from hPSC-mesenchyme after co-culture in the presence of human JAG1 blocking antibody or control goat IgG (*p < 0.05, **p < 0.01, n = 3 independent experiments).

(E) Expression of WNT inhibitors *SFRP1*, *SFRP2*, and *DKK1* in $CD146^{hi}CD73^{hi}$ and $CD146^{lo}CD73^{lo}$ mesenchyme (n = 3 biological replicates, RNA-seq **FDR < 0.01, ***FDR < 0.001).

(F) qRT-PCR of WNT target genes *TCF7* and *LEF1* in Lin^{+} cells recovered from $CD146^{hi}CD73^{hi}$ and $CD146^{lo}CD73^{lo}$ mesenchyme after 7 days of co-culture without extra cytokines (n = 5 biological replicates, *p < 0.05).

(G) $CD34^{+}$ Lin^{-}, myeloid and lymphoid cell numbers after activation of Wnt signaling by addition of 3 μM CHIR99021 (*p < 0.05, **p < 0.01, ***p < 0.001; ns, not significant; n = 3 independent experiments).

Error bars represent SEM. See also Figure S4.

(CHIR), promoted rapid differentiation into both myeloid and lymphoid lineages, and loss of $CD34^{+}Lin^{-}$ cells in both $CD146^{hi}CD73^{hi}$ and $CD146^{lo}CD73^{lo}$ co-cultures (Figure 3G). This latter observation is consistent with previous findings that canonical Wnt signaling regulates hematopoiesis in a dosage-dependent fashion, with high Wnt activation detrimental to HSC self-renewal leading to depletion of the LT-HSC pool (Famili et al., 2016; Luis et al., 2011). It is possible that functional redundancy among Wnt inhibitors obscures the impact of manipulating expression of single factors such as SFRP1 on HSPC support during co-culture.

hPSC-Derived CD146^{hi}CD73^{hi} Mesenchyme Shares a Coordinated Gene Expression Profile that Resembles that of Primary Human Pericytes

Given the complexity of signals produced in the HSC niche, it seems likely that no single factor or mechanism mediates the differential support of hematopoiesis from different mesenchymal subpopulations. As molecular characterization and functional studies of hPSC-derived CD146^{hi}CD73^{hi} and CD146^{lo}CD73^{lo} mesenchyme showed strong parallels to populations from primary human tissue, we performed comparative transcriptome analysis of each phenotypic population derived from hPSCs with those from primary adipose tissue (freshly isolated or after culture).

Principal-component analysis showed that the populations clustered mostly based on source rather than immunophenotype (data not shown). Similar observations that tissue-imprinted genes constitute major variances in unsupervised analysis have been reported in other comparative studies (Charbord et al., 2014). To uncover shared functional gene sets across stromal lines with HSPC-supportive capacity, we performed gene set enrichment analysis (Subramanian et al., 2005) as follows. The most up- and downregulated genes in hPSC-CD146^{hi}CD73^{hi} cells (compared with hPSC-CD146^{lo}CD73^{lo} cells) were defined as *positive* and *negative signatures*, respectively (FDR < 0.01 and at least 2-fold difference). These signatures of hPSC-derived CD146^{hi}CD73^{hi} cells were compared with the global expression profiles of primary CD146^{+} pericytes, ranked by differential expression to primary CD146^{-} cells. Significant enrichment was found between the positive signatures of hPSC-derived CD146^{hi}CD73^{hi} cells with genes upregulated in adult pericytes (Figure 4A, enrichment score of 1.36 and 1.78 in fresh and cultured pericytes respectively). Similarly, the negative signatures of hPSC-CD146^{hi}CD73^{hi} cells were significantly enriched in genes highly downregulated in primary pericytes (Figure 4B, enrichment score of −1.77 and −1.39). Thus hPSC- and adipose-derived CD146^{hi}CD73^{hi} cells exhibited similar transcriptional signatures.

The shared core transcriptional signature obtained from both hPSC- and adipose-derived CD146^{++} cells (104 genes, Table S1) was imported into the STRING database to identify known and predicted protein interactions (STRING protein-protein interaction enrichment $p < 10 \times 10^{-12}$) (Figure 4C). Of note, the dominant functional categories identified in the STRING analysis were those enriched in biological processes characteristic of pericytes, i.e., cell adhesion (FDR < 6×10^{-6}), vasculature development (FDR < 7×10^{-8}), regulation of cell motion (FDR < 3×10^{-8}), and wound healing (FDR < 3×10^{-4}), among others (Figure 4C). Therefore, the shared transcriptional signature between hPSC- and adipose-derived CD146^{++} cells is significantly enriched in processes involved in niche homeostasis and maintenance.

DISCUSSION

Mesenchymal stromal/stem cells, either derived from primary tissues or differentiated from hPSC, are conventionally isolated and expanded as a population of cells loosely defined by CD73, CD105, and CD90 expression (Murray et al., 2014). Our data strongly argue that phenotypically, molecularly, and functionally distinct populations coexist within these conventional definitions of mesenchymal stroma. Previously, CD146 was shown to define mesenchymal precursors adjacent to the vasculature of multiple human organs, including bone marrow and adipose tissues (Crisan et al., 2009). Other studies have derived CD146^{+} pericytes from hPSCs, demonstrating the capacity of these cells to reconstruct a vascular network (Dar et al., 2012; Kusuma et al., 2013; Orlova et al., 2014). Our previous work (Corselli et al., 2013) identified immunophenotypic subsets of mesenchyme isolated from human primary tissues and found that a subpopulation of perivascular mesenchyme with high expression of CD146 possessed significantly greater HSPC supporting ability. In the current paper, we show that two phenotypically, functionally, and molecularly distinct mesenchymal populations can be faithfully recapitulated in the hPSC system. We also provide the transcriptome profiling of these mesenchymal populations, revealing the HSPC-supportive CD146^{hi}CD73^{hi} cells to be closely related to primary pericytes.

hPSC-derived CD146^{hi}CD73^{hi} mesenchyme showed high expression of *NES*, *LEPR*, and *CSPG4*, markers of peri-sinusoidal and peri-arteriolar cells in the murine HSC niche (Ding et al., 2012; Kunisaki et al., 2013; Méndez-Ferrer et al., 2010; Zhou et al., 2014). The relevance of these perivascular cells has recently been addressed in the context of human hematopoiesis (Corselli et al., 2013; Pinho et al., 2013). PDGFRα/CD140a, which is a long-known marker for murine mesenchymal stromal cells (MSCs), was also reported on human fetal bone marrow MSCs capable of supporting HSPC expansion (Pinho et al., 2013). In contrast, later studies using adult human bone marrow reported that MSCs with hematopoiesis-supporting ability were highly enriched within the CD140a$^{lo/-}$ population but not in CD140a^{+} cells (Li et al., 2014). These conflicting results may be explained by reports of human mesenchymal stroma, including our own (Corselli et al., 2013), which suggest that CD140a expression is differentially regulated both developmentally and across tissue types. A recent report demonstrated that nestin^{+} mesenchyme in the

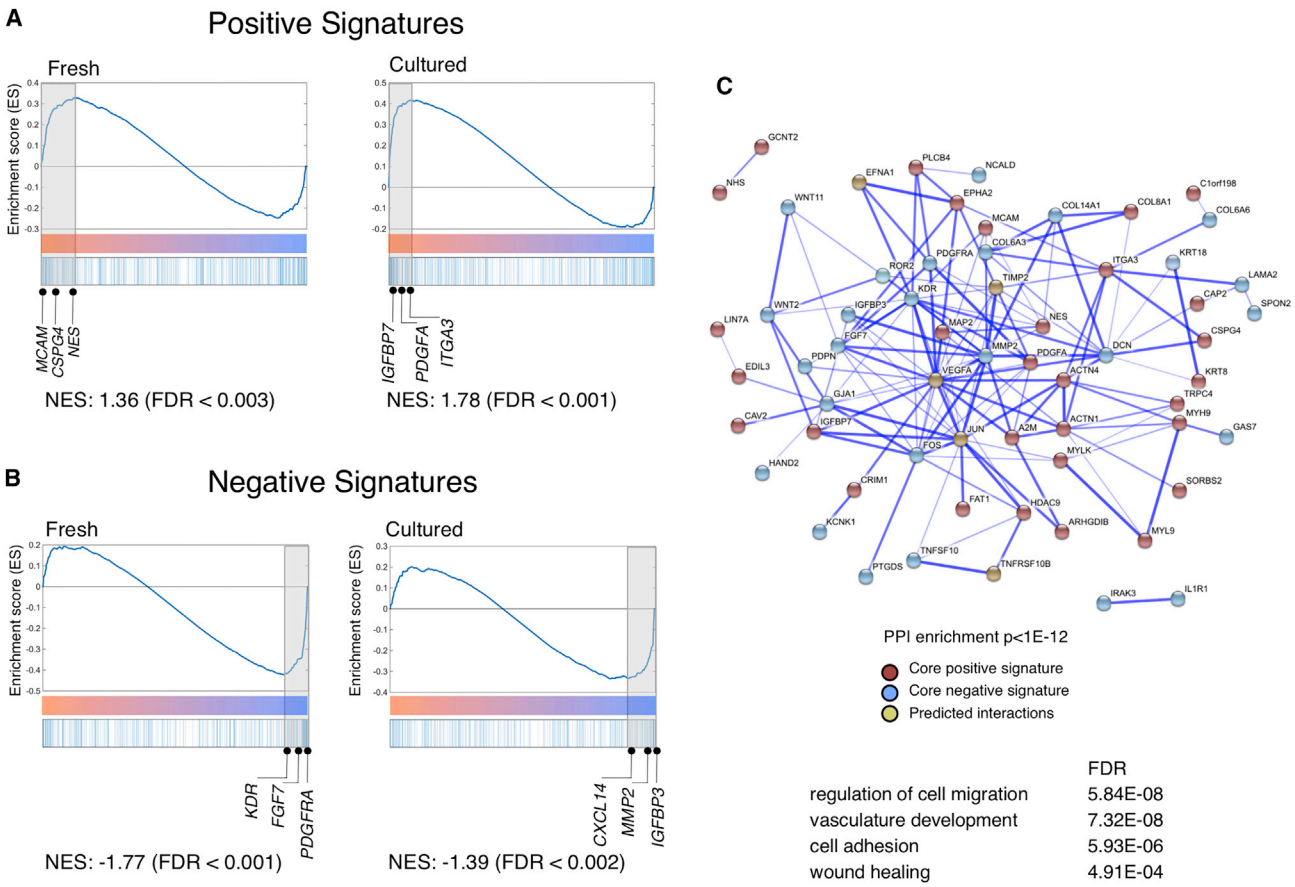

Figure 4. hPSC-Derived CD146^{hi}CD73^{hi} Mesenchyme Shares a Molecular Signature with Primary Human Adult Pericytes

(A and B) Gene set enrichment analysis of hPSC-derived mesenchyme and lipoaspirate-derived populations (both freshly sorted and cultured). (A) Positive and (B) negative signatures were defined, respectively, as up- and downregulated genes in hPSC-derived CD146^{hi}CD73^{hi} compared with hPSC-derived CD146^{lo}CD73^{lo} cells. The x axis represents genes ranked from positive to negative fold change in lipoaspirate-CD146^{+} compared with lipoaspirate-CD146^{-} cells. Genes in the core enrichment set are highlighted (shaded gray boxes) and selected genes in this core enrichment set are shown.

(C) Up- and downregulated genes common to the core sets of CD146^{hi} from hPSC and fresh and cultured primary CD146^{+} cells were imported into the STRING database, which identified a network of known protein-protein interactions (enrichment p value = 0), along with a number of high-confidence (score > 0.9999) predicted interactions. Line thickness is proportional to the confidence level of each interaction. See also Table S1.

murine fetal liver HSC niche expressed CD146 (Khan et al., 2016), further supporting the inclusion of CD146 in defining mesenchyme with HSC niche activity.

In the present study, both CD146^{hi}CD73^{hi} and CD146^{lo}CD73^{lo} cells from hPSCs expressed known HSC niche genes, such as *SLIT2* and *ANGPT1*. However, other niche factors, such as *KITL*, *JAG1*, and *IGFBP2*, were specifically upregulated in CD146^{hi}CD73^{hi} cells. As is likely for the components of the hematopoietic niche *in vivo*, we conclude the CD146^{hi}CD73^{hi} mesenchymal subset supports HSPCs through a combination of mechanisms that involve cell-cell contact (e.g., Notch signaling and adhesion molecules) and secreted factors (e.g., Wnt regulators and cytokines). Time course analysis for the development of CD146^{hi}CD73^{hi} and CD146^{lo}CD73^{lo} cells showed that they could each be distinguished early during mesenchymal differentiation. However, clonal data are needed to understand the developmental relationships of these cell types. It should also be acknowledged that it remains unclear whether the phenotypes examined in our study represent cell types at the extremes of a functional spectrum.

The identification of distinct mesenchymal subsets generated from hPSCs provides a foundation from which developmental and functional differences can be further defined, and the application of each population for cell therapy explored. The ability to prospectively isolate human stroma with HSC-supporting capacity is

particularly relevant given clinical interest in using stroma co-culture as a platform for HSC expansion (Hofmeister et al., 2007).

While this study focused on defining cellular subsets within hPSC-derived mesenchyme that would support a well-characterized HSPC population, the existence of distinct mesenchymal subsets during hPSC differentiation has broader implication for the directed differentiation of hPSCs toward definitive, functional HSCs. Further study will be needed to define the optimal hPSC-derived mesenchyme that would promote HSC specification.

EXPERIMENTAL PROCEDURES

Mesoderm Differentiation from hPSCs to Generate hEMPs

The hPSC lines H1 (WiCell, Madison, WI), and UCLA3 and UCLA6 (UCLA BSCRC hESC Core) were maintained and expanded on irradiated primary mouse embryonic fibroblasts (EMD Millipore, Billerica, MA). All hPSC experiments were approved by the UCLA Embryonic Stem Cell Research Oversight (ESCRO) committee. Mesoderm commitment was induced as described previously (Evseenko et al., 2010; Hoffman and Calvi, 2014) (Supplemental Experimental Procedures). $CD326^{-}CD56^{+}$ embryonic mesoderm progenitors (hEMPs) were isolated by flow cytometry at day 3.5 (Figure 1A) and seeded onto Matrigel for mesenchymal differentiation over the next 14 days.

Mesenchymal Differentiation from hEMPs

To induce mesenchymal differentiation, hEMPs were seeded at 50,000 cells/well into 6-well tissue culture plates, pre-coated with Matrigel. Day 0–7 of differentiation, MesenCult Proliferation Kit, Human (STEMCELL Technologies) supplemented with SB-431542 (10 μM, R&D Systems) was used. Day 0–3, 10 μM Rock inhibitor (Y27632 hydrochloride; R&D Systems) and 10 μg/mL gentamicin (Gibco, Thermo Fisher Scientific, Waltham, MA) were also added. Day 7–14, medium was switched to EGM-2 (Lonza) supplemented with SB-431542 (10 μM). Day 14–18, cells were dissociated into single-cell suspension with Accutase (Innovative Cell Technologies, San Diego, CA), and analyzed or isolated by fluorescence-activated cell sorting (FACS) (see Supplemental Experimental Procedures).

Co-culture of Stromal Cells and CB $CD34^{+}$ Cells

hEMP-derived mesenchyme ($CD146^{hi}CD73^{hi}$ and $CD146^{lo}CD73^{lo}$) was isolated from mesenchymal cultures after 14–18 days and re-plated in 96-well tissue culture-treated plates at 6.5×10^3 cells per well in 100 μL of EGM-2. Three days later, CB $CD34^{+}$ cells (>80% purity, 1×10^5 per well) were plated on 80% confluent stroma in 200 μL of co-culture medium consisting of RPMI 1640, L-glutamine, 5% fetal bovine serum, and penicillin/streptavidin. No supplemental cytokines were added unless otherwise indicated ($Lin^{-}CD34^{+}CD38^{-}$ experiments). Cells were harvested after 2 weeks unless otherwise indicated for FACS analysis, CFU assay, and *in vivo* repopulating assay.

Graphical and Statistical Analysis

Graphs were generated and statistics analyzed using GraphPad Prism software. Paired parametric two-tailed t tests were used to calculate p values except in cases where normalized values were used, in which case unpaired parametric t tests were used. $p < 0.05$ was considered statistically significant.

ACCESSION NUMBERS

The accession numbers for the RNA sequence data reported in this paper are GEO: GSE77879 and GSE83443.

SUPPLEMENTAL INFORMATION

Supplemental Information includes Supplemental Experimental Procedures, four figures, and one table and can be found with this article online at https://doi.org/10.1016/j.stemcr.2017.12.005.

AUTHOR CONTRIBUTIONS

C.J.C. and S.L., conception and design, collection and assembly of data, data analysis and interpretation, and manuscript writing. M.C., conception and design and collection of data. D.C., RNA-seq data analysis and interpretation. Y.Z. and C.B.H., collection of data. R.H. and B.P., RNA-seq data collection. G.M.C., conception and design, data analysis and interpretation, manuscript writing, financial support, and final approval of manuscript.

ACKNOWLEDGMENT

We thank J. Scholes and F. Codrea at the UCLA Broad Stem Cell Research Center (BSCRC) Flow Cytometry Core for assistance with cell sorting and R. Chan for assistance with specimen processing. The research was made possible by grants from the California Institute of Regenerative Medicine (CIRM), grant numbers RB3-05217 (to G.M.C.) and TR2-01821 (to B.P.). C.J.C. and M.C. acknowledge the support of the California Institute for Regenerative Medicine Training Grant (TG2-01169), and S.L. acknowledges the support of a fellowship grant from the UCLA BSCRC Training Program. Core services were supported by the Genomics Shared Resource (GSR) in the UCLA Jonsson Comprehensive Cancer Center (NIH/NCI 5P30CA016042), the BSCRC Flow Cytometry Core, and the UCLA Center for AIDS Research (CFAR) Virology Core Lab (NIH/NIAID AI028697).

Received: May 29, 2016
Revised: December 4, 2017
Accepted: December 5, 2017
Published: January 4, 2018

REFERENCES

Charbord, P., Pouget, C., Binder, H., Dumont, F., Stik, G., Levy, P., Allain, F., Marchal, C., Richter, J., Uzan, B., et al. (2014). A systems biology approach for defining the molecular framework of the hematopoietic stem cell niche. Cell Stem Cell *15*, 376–391.

Chin, C.J., Cooper, A.R., Lill, G.R., Evseenko, D., Zhu, Y., He, C.B., Casero, D., Pellegrini, M., Kohn, D.B., and Crooks, G.M. (2016). Genetic tagging during human mesoderm differentiation reveals

tripotent lateral plate mesodermal progenitors. Stem Cells *34*, 1239–1250.

Corselli, M., Chin, C.J., Parekh, C., Sahaghian, A., Wang, W., Ge, S., Evseenko, D., Wang, X., Montelatici, E., Lazzari, L., et al. (2013). Perivascular support of human hematopoietic stem/progenitor cells. Blood *121*, 2891–2901.

Crisan, M., Chen, C.W., Corselli, M., Andriolo, G., Lazzari, L., and Péault, B. (2009). Perivascular multipotent progenitor cells in human organs. Ann. N. Y. Acad. Sci. *1176*, 118–123.

Crisan, M., Yap, S., Casteilla, L., Chen, C.W., Corselli, M., Park, T.S., Andriolo, G., Sun, B., Zheng, B., Zhang, L., et al. (2008). A perivascular origin for mesenchymal stem cells in multiple human organs. Cell Stem Cell *3*, 301–313.

Dar, A., Domev, H., Ben-Yosef, O., Tzukerman, M., Zeevi-Levin, N., Novak, A., Germanguz, I., Amit, M., and Itskovitz-Eldor, J. (2012). Multipotent vasculogenic pericytes from human pluripotent stem cells promote recovery of murine ischemic limb. Circulation *125*, 87–99.

Ding, L., Saunders, T.L., Enikolopov, G., and Morrison, S.J. (2012). Endothelial and perivascular cells maintain haematopoietic stem cells. Nature *481*, 457–462.

Evseenko, D., Zhu, Y., Schenke-Layland, K., Kuo, J., Latour, B., Ge, S., Scholes, J., Dravid, G., Li, X., MacLellan, W.R., et al. (2010). Mapping the first stages of mesoderm commitment during differentiation of human embryonic stem cells. Proc. Natl. Acad. Sci. USA *107*, 13742–13747.

Famili, F., Brugman, M.H., Taskesen, E., Naber, B.E., Fodde, R., and Staal, F.J. (2016). High levels of canonical Wnt signaling lead to loss of stemness and increased differentiation in hematopoietic stem cells. Stem Cell Reports *6*, 652–659.

Ferrell, P.I., Hexum, M.K., Kopher, R.A., Lepley, M.A., Gussiaas, A., and Kaufman, D.S. (2014). Functional assessment of hematopoietic niche cells derived from human embryonic stem cells. Stem Cells Dev. *23*, 1355–1363.

Greenbaum, A., Hsu, Y.M., Day, R.B., Schuettpelz, L.G., Christopher, M.J., Borgerding, J.N., Nagasawa, T., and Link, D.C. (2013). CXCL12 in early mesenchymal progenitors is required for haematopoietic stem-cell maintenance. Nature *495*, 227–230.

Hoffman, C.M., and Calvi, L.M. (2014). Minireview: complexity of hematopoietic stem cell regulation in the bone marrow microenvironment. Mol. Endocrinol. *28*, 1592–1601.

Hofmeister, C.C., Zhang, J., Knight, K.L., Le, P., and Stiff, P.J. (2007). Ex vivo expansion of umbilical cord blood stem cells for transplantation: growing knowledge from the hematopoietic niche. Bone Marrow Transpl. *39*, 11–23.

Huynh, H., Iizuka, S., Kaba, M., Kirak, O., Zheng, J., Lodish, H.F., and Zhang, C.C. (2008). Insulin-like growth factor-binding protein 2 secreted by a tumorigenic cell line supports ex vivo expansion of mouse hematopoietic stem cells. Stem Cells *26*, 1628–1635.

Itkin, T., Gur-Cohen, S., Spencer, J.A., Schajnovitz, A., Ramasamy, S.K., Kusumbe, A.P., Ledergor, G., Jung, Y., Milo, I., Poulos, M.G., et al. (2016). Distinct bone marrow blood vessels differentially regulate haematopoiesis. Nature *532*, 323–328.

Khan, J.A., Mendelson, A., Kunisaki, Y., Birbrair, A., Kou, Y., Arnal-Estapé, A., Pinho, S., Ciero, P., Nakahara, F., Ma'ayan, A., et al. (2016). Fetal liver hematopoietic stem cell niches associate with portal vessels. Science *351*, 176–180.

Kobayashi, H., Butler, J.M., O'Donnell, R., Kobayashi, M., Ding, B.S., Bonner, B., Chiu, V.K., Nolan, D.J., Shido, K., Benjamin, L., et al. (2010). Angiocrine factors from Akt-activated endothelial cells balance self-renewal and differentiation of haematopoietic stem cells. Nat. Cell Biol. *12*, 1046–1056.

Kunisaki, Y., Bruns, I., Scheiermann, C., Ahmed, J., Pinho, S., Zhang, D., Mizoguchi, T., Wei, Q., Lucas, D., Ito, K., et al. (2013). Arteriolar niches maintain haematopoietic stem cell quiescence. Nature *502*, 637–643.

Kusuma, S., Shen, Y.I., Hanjaya-Putra, D., Mali, P., Cheng, L., and Gerecht, S. (2013). Self-organized vascular networks from human pluripotent stem cells in a synthetic matrix. Proc. Natl. Acad. Sci. USA *110*, 12601–12606.

Li, H., Ghazanfari, R., Zacharaki, D., Ditzel, N., Isern, J., Ekblom, M., Méndez-Ferrer, S., Kassem, M., and Scheding, S. (2014). Low/negative expression of PDGFR-α identifies the candidate primary mesenchymal stromal cells in adult human bone marrow. Stem Cell Reports *3*, 965–974.

Luis, T.C., Naber, B.A., Roozen, P.P., Brugman, M.H., de Haas, E.F., Ghazvini, M., Fibbe, W.E., van Dongen, J.J., Fodde, R., and Staal, F.J. (2011). Canonical wnt signaling regulates hematopoiesis in a dosage-dependent fashion. Cell Stem Cell *9*, 345–356.

Murray, I.R., West, C.C., Hardy, W.R., James, A.W., Park, T.S., Nguyen, A., Tawonsawatruk, T., Lazzari, L., Soo, C., and Péault, B. (2014). Natural history of mesenchymal stem cells, from vessel walls to culture vessels. Cell Mol. Life Sci. *71*, 1353–1374.

Méndez-Ferrer, S., Lucas, D., Battista, M., and Frenette, P.S. (2008). Haematopoietic stem cell release is regulated by circadian oscillations. Nature *452*, 442–447.

Méndez-Ferrer, S., Michurina, T.V., Ferraro, F., Mazloom, A.R., Macarthur, B.D., Lira, S.A., Scadden, D.T., Ma'ayan, A., Enikolopov, G.N., and Frenette, P.S. (2010). Mesenchymal and haematopoietic stem cells form a unique bone marrow niche. Nature *466*, 829–834.

Nakamura-Ishizu, A., Okuno, Y., Omatsu, Y., Okabe, K., Morimoto, J., Uede, T., Nagasawa, T., Suda, T., and Kubota, Y. (2012). Extracellular matrix protein tenascin-C is required in the bone marrow microenvironment primed for hematopoietic regeneration. Blood *119*, 5429–5437.

Orlova, V.V., Drabsch, Y., Freund, C., Petrus-Reurer, S., van den Hil, F.E., Muenthaisong, S., Dijke, P.T., and Mummery, C.L. (2014). Functionality of endothelial cells and pericytes from human pluripotent stem cells demonstrated in cultured vascular plexus and zebrafish xenografts. Arterioscler. Thromb. Vasc. Biol. *34*, 177–186.

Pinho, S., Lacombe, J., Hanoun, M., Mizoguchi, T., Bruns, I., Kunisaki, Y., and Frenette, P.S. (2013). PDGFRα and CD51 mark human nestin+ sphere-forming mesenchymal stem cells capable of hematopoietic progenitor cell expansion. J. Exp. Med. *210*, 1351–1367.

Poulos, M.G., Guo, P., Kofler, N.M., Pinho, S., Gutkin, M.C., Tikhonova, A., Aifantis, I., Frenette, P.S., Kitajewski, J., Rafii, S.,

et al. (2013). Endothelial Jagged-1 is necessary for homeostatic and regenerative hematopoiesis. Cell Rep. *4*, 1022–1034.

Sacchetti, B., Funari, A., Michienzi, S., Di Cesare, S., Piersanti, S., Saggio, I., Tagliafico, E., Ferrari, S., Robey, P.G., Riminucci, M., et al. (2007). Self-renewing osteoprogenitors in bone marrow sinusoids can organize a hematopoietic microenvironment. Cell *131*, 324–336.

Subramanian, A., Tamayo, P., Mootha, V.K., Mukherjee, S., Ebert, B.L., Gillette, M.A., Paulovich, A., Pomeroy, S.L., Golub, T.R., Lander, E.S., et al. (2005). Gene set enrichment analysis: a knowledge-based approach for interpreting genome-wide expression profiles. Proc. Natl. Acad. Sci. USA *102*, 15545–15550.

Vodyanik, M.A., Yu, J., Zhang, X., Tian, S., Stewart, R., Thomson, J.A., and Slukvin, I.I. (2010). A mesoderm-derived precursor for mesenchymal stem and endothelial cells. Cell Stem Cell *7*, 718–729.

Zhang, C.C., Kaba, M., Iizuka, S., Huynh, H., and Lodish, H.F. (2008). Angiopoietin-like 5 and IGFBP2 stimulate ex vivo expansion of human cord blood hematopoietic stem cells as assayed by NOD/SCID transplantation. Blood *111*, 3415–3423.

Zhou, B.O., Yue, R., Murphy, M.M., Peyer, J.G., and Morrison, S.J. (2014). Leptin-receptor-expressing mesenchymal stromal cells represent the main source of bone formed by adult bone marrow. Cell Stem Cell *15*, 154–168.

Stem Cell Reports, Volume *10*

Supplemental Information

Transcriptionally and Functionally Distinct Mesenchymal Subpopulations Are Generated from Human Pluripotent Stem Cells

Chee Jia Chin, Suwen Li, Mirko Corselli, David Casero, Yuhua Zhu, Chong Bin He, Reef Hardy, Bruno Péault, and Gay M. Crooks

Figure S1

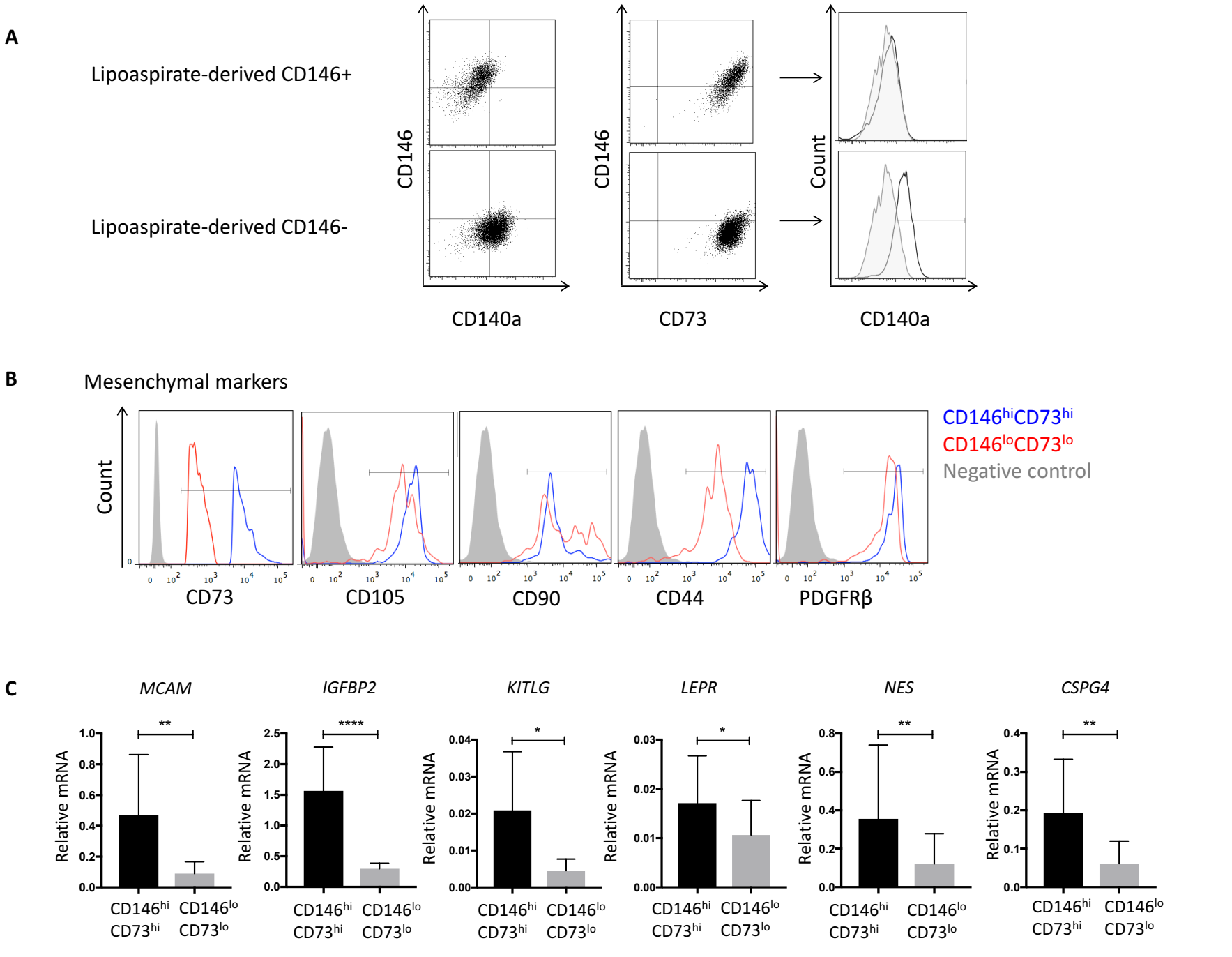
A
Lipoaspirate-derived CD146+
Lipoaspirate-derived CD146-
CD146
CD140a
CD146
CD73
Count
CD140a
B
Mesenchymal markers
Count
CD73
CD105
CD90
CD44
PDGFRβ
CD146hiCD73hi
CD146loCD73lo
Negative control
C
MCAM
IGFBP2
KITLG
LEPR
NES
CSPG4
Relative mRNA
**
****
*
*
**
**
CD146hi CD73hi
CD146lo CD73lo

Fig S1. Immunophenotypic and molecular characterization of primary and hPSC-derived mesenchymal cells. Related to Fig 1. (A) Inverse relationship of CD146 and CD73 to CD140a on mesenchymal cells from primary human tissue are similar to hPSC derived mesenchyme. Flow cytometry analysis of lipoaspirate-derived $CD146^{+}$ and $CD146^{-}$ cells, purified and cultured (passage 5-13). Unstained control shown shaded in grey. Representative data from 3 biological replicates. **(B)** $CD146^{hi}CD73^{hi}$ and $CD146^{lo}CD73^{lo}$ cells express conventional mesenchymal markers. H1 hEMP-derived mesenchymal cultures were analyzed at week 2 by FACS. All cells were gated as $CD31^{neg}$ and then either $CD146^{hi}CD73^{hi}$ (blue) or $CD146^{lo}CD73^{lo}$ (red). Data are representative of 4 independent analyses. **(C)** Expression of genes associated with the HSPC niche is enriched in the $CD146^{hi}CD73^{hi}$ population. Quantitative RT-PCR of RNA from $CD146^{hi}CD73^{hi}$ and $CD146^{lo}CD73^{lo}$ cells (means and SEM shown, n= 4-6 independent experiments. * $p<0.05$, ** $p<0.01$, *** $p<0.001$, **** $p<0.0001$; paired Student's t test.

Figure S2

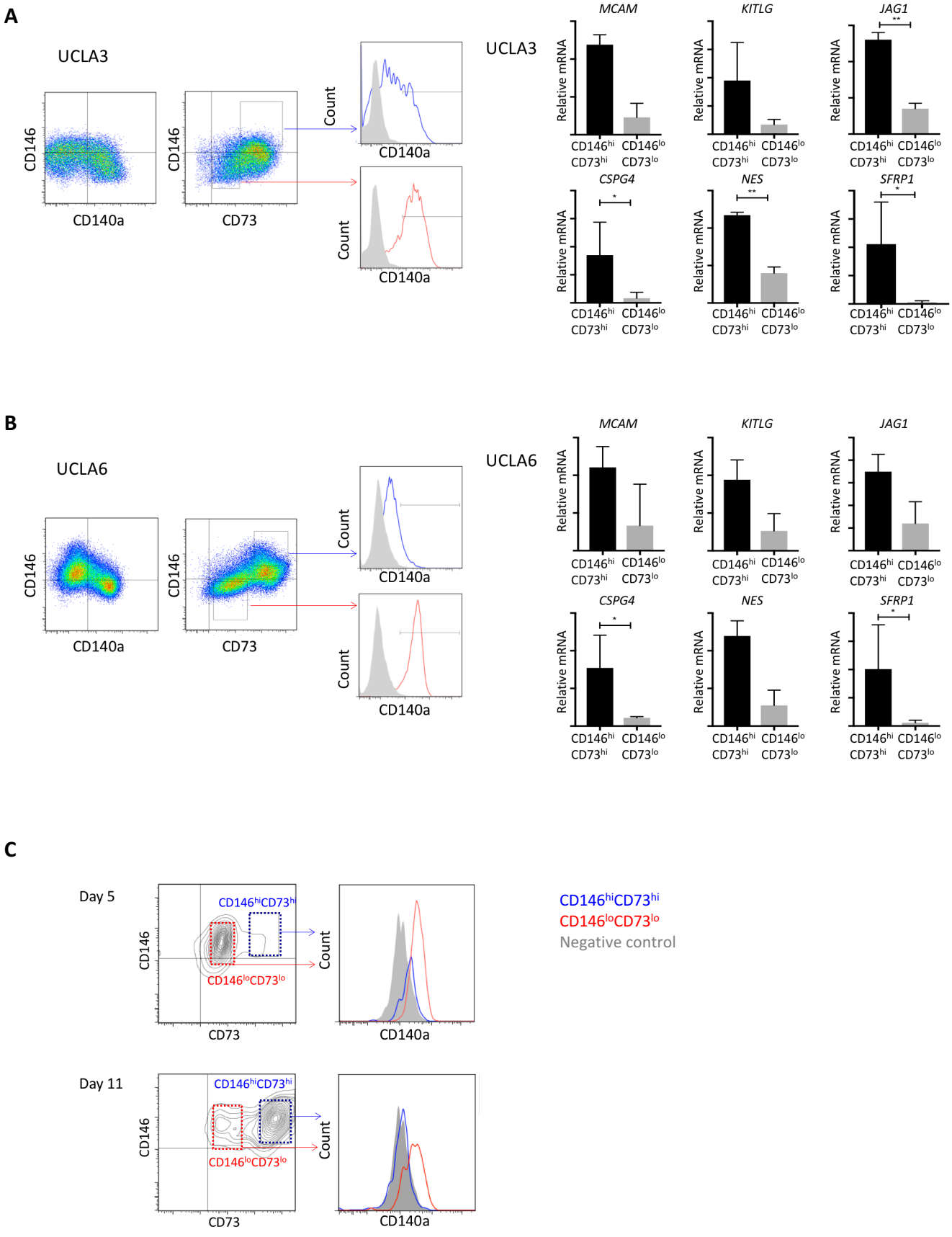
A
UCLA3
CD146
CD140a
CD146
CD73
Count
CD140a
Count
CD140a
UCLA3
MCAM
KITLG
JAG1
CSPG4
NES
SFRP1
Relative mRNA
CD146hi CD73hi
CD146lo CD73lo
B
UCLA6
CD146
CD140a
CD146
CD73
Count
CD140a
Count
CD140a
UCLA6
MCAM
KITLG
JAG1
CSPG4
NES
SFRP1
Relative mRNA
CD146hi CD73hi
CD146lo CD73lo
C
Day 5
CD146hiCD73hi
CD146loCD73lo
CD146
CD73
Count
CD140a
Day 11
CD146hiCD73hi
CD146loCD73lo
CD146
CD73
Count
CD140a
CD146hiCD73hi
CD146loCD73lo
Negative control

Fig S2. Consistency of immunophenotype and gene expression in mesenchymal subsets from additional hPSC lines and at different times during differentiation. Related to Fig 1. (A) and **(B)** Mesenchymal populations generated from two additional hESC lines demonstrate similar immunophenotype and gene expression to H1. Mesenchymal differentiation was initiated from hEMP generated from the hESC lines **(A)** UCLA3 and **(B)** UCLA6, and then analyzed after 2 weeks by Flow cytometry (representative of n=2 biological replicates per cell line) and quantitative RT-PCR (mean and SEM shown, n= 2-3 independent experiments) * $p<0.05$, ** $p<0.01$; paired two-tailed Student's t test. **(C)** Distinct mesenchymal populations with an inverse relationship of CD73 and CD140a are detectable early on during the differentiation from hEMP. Flow cytometry analysis of differentiation cultures from hEMP showed that two mesenchymal populations distinguished by CD73 expression were detected as early as day 5 of differentiation. As with later stages of differentiation, the $CD73^{++}$ population was $CD140a^{-}$ while the $CD73^{+}$ population was $CD140a^{+}$. Fluorescent minus one (FMO) for CD140a-PE was used to set gates. All cells were first gated as $CD31^{neg}$. Representative data from 3 biological replicates.

Figure S3

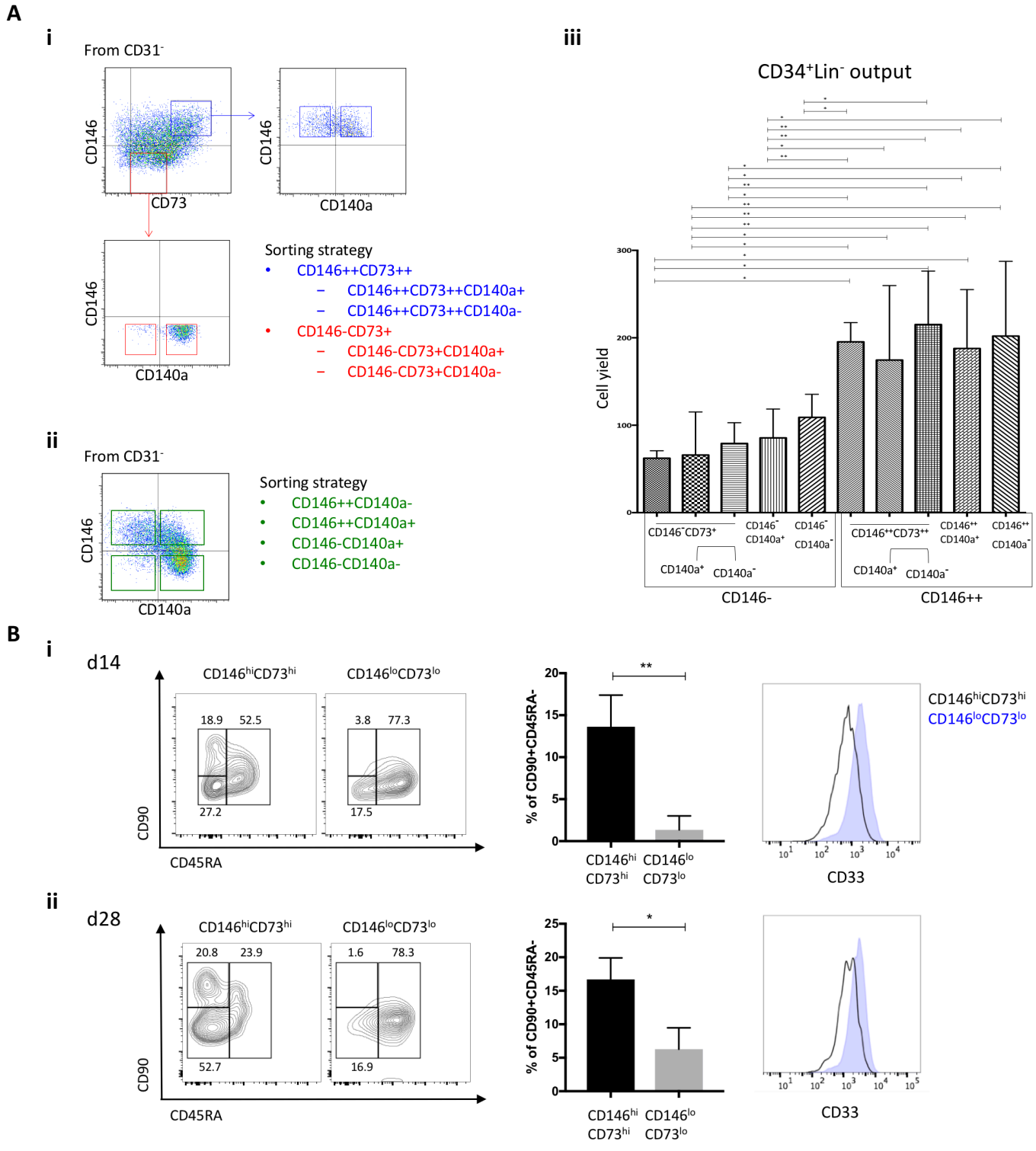
A
i
From CD31-
CD146
CD73
CD140a
Sorting strategy
CD146++CD73++
CD146++CD73++CD140a+
CD146++CD73++CD140a-
CD146-CD73+
CD146-CD73+CD140a+
CD146-CD73+CD140a-
ii
From CD31-
Sorting strategy
CD146++CD140a-
CD146++CD140a+
CD146-CD140a+
CD146-CD140a-
iii
CD34+Lin- output
Cell yield
CD146-
CD146++
B
i
d14
CD146hiCD73hi
CD146loCD73lo
18.9
52.5
27.2
3.8
77.3
17.5
CD90
CD45RA
% of CD90+CD45RA-
CD33
ii
d28
20.8
23.9
52.7
1.6
78.3
16.9

Fig S3. Analyses of alternative mesenchymal and hematopoietic populations. Related to Fig 2. (A) CD146 expression of hPSC-derived mesenchyme defines HSPC supportive capacity. Multiple different CD31- subpopulations were purified after two-week mesenchymal differentiation from H1 hEMP and tested for their ability to support HSPC *ex vivo*. **(i)** Initial gating on CD146 v CD73, then subdivided based on CD140a expression. **(ii)** Alternative gating strategy on CD146 v CD140a without CD73. **(iii)** High CD146 expression best served as a distinguishing cell surface marker to identify HSPC-supporting stroma based on CD34+lin- yield per 1000 initially seeded CD34+ cells (means and SEM shown, n=3 biological replicates, * $p<0.05$, ** $p<0.01$; unpaired two-tailed Student's t test). **(B) $CD146^{hi}CD73^{hi}$ mesenchyme supports ex *vivo* maintenance of HSC.** CD34+CD38-Lin- CB cells were isolated by flow cytometry and co-cultured on either $CD146^{hi}CD73^{hi}$ or $CD146^{lo}CD73^{lo}$ mesenchymal cells generated from H1-derived hEMP in 5% serum with the addition of Fms-related tyrosine kinase 3 ligand (50ng/ml) and thrombopoietin (50ng/ml). After **(i)** 14 or **(ii)** 28 days, hematopoietic cells were harvested and analyzed by flow cytometry. FACS plots shown were first gated on live (DAPI-) Lin-CD34+ cells. Bar graphs show the percentage of live Lin-CD34+ cells that were CD90+CD45RA- by flow cytometry at each time point (mean and SEM shown, n=4 biological replicates, * $p<0.05$, ** $p<0.01$; paired two-tailed Student's t test). On the right is the expression of CD33 of the Lin-CD34+ cells from co-cultures. $CD146^{hi}CD73^{hi}$ shown as solid black line and $CD146^{lo}CD73^{lo}$ shown as shaded. **(C) $CD146^{hi}CD73^{hi}$ mesenchyme supports engraftable HSPCs.** Bone marrow engraftment (% human cells) of mice 6 weeks after primary and secondary transplants. CB $CD34^{+}$ cells were co-cultured with $CD146^{hi}CD73^{hi}$ or $CD146^{lo}CD73^{lo}$ monolayers for 2 weeks. An equal number of $CD45^{+}$ cells (1×10^{5}) harvested from each co-culture was intratibially injected into each sublethally irradiated (250 cGy), 6- to 8-week-old NSG mouse (The Jackson Laboratory). Control animals received 1×10^{5} cells fresh, enriched CD34+ cells from the same CB (CB w/o culture). (means and SEM shown, n = 5 independent experiments, total 9-14 mice per group; ***P <0.0001).

Figure S4

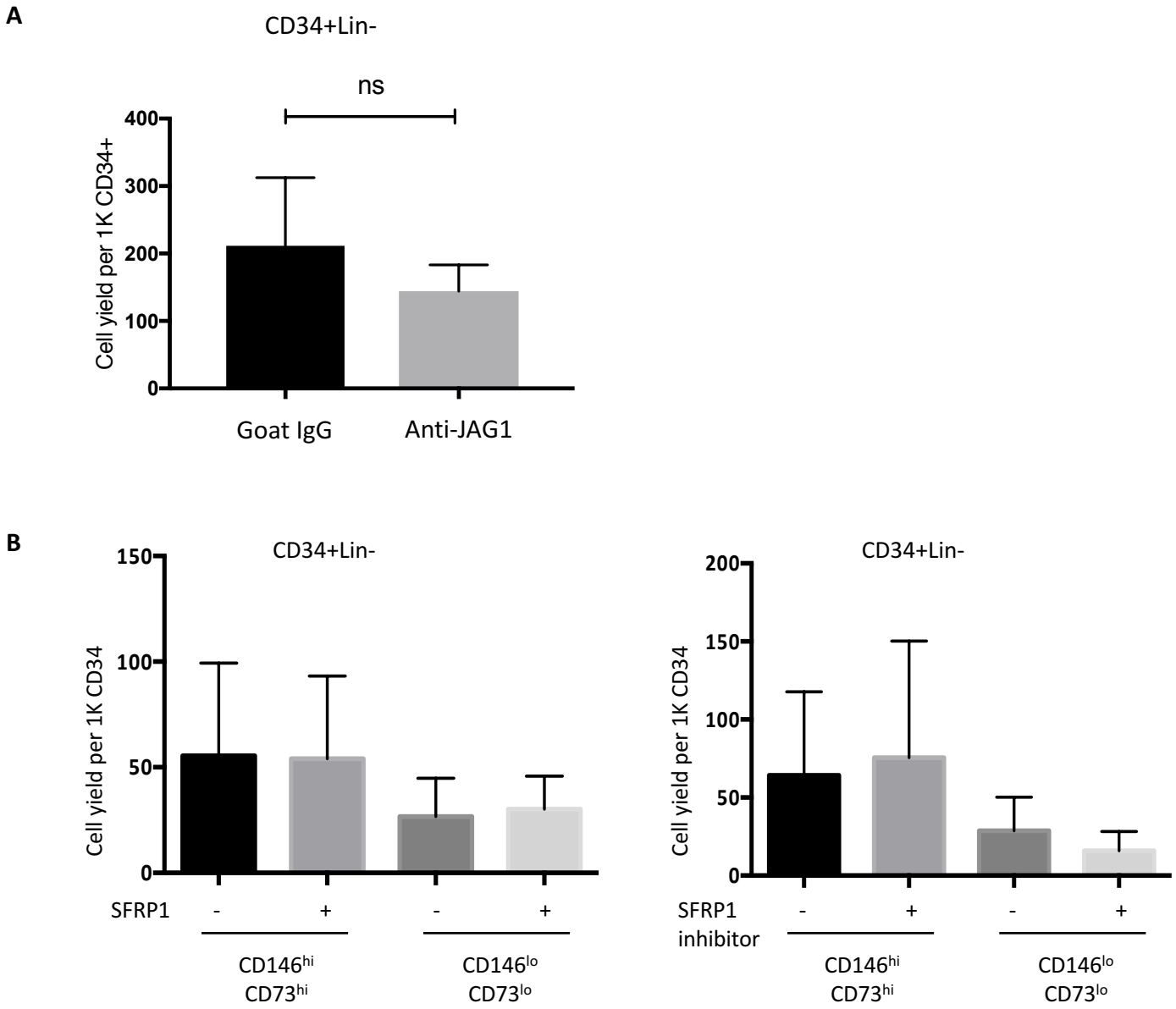
A
CD34+Lin-
ns
Cell yield per 1K CD34+
400
300
200
100
0
Goat IgG
Anti-JAG1
B
CD34+Lin-
Cell yield per 1K CD34
150
100
50
0
SFRP1
-
+
-
+
CD146hi
CD73hi
CD146lo
CD73lo
CD34+Lin-
Cell yield per 1K CD34
200
150
100
50
0
SFRP1
inhibitor
-
+
-
+
CD146hi
CD73hi
CD146lo
CD73lo

Fig S4. Mechanisms of HSPC support of hPSC-derived mesenchymes. Related to Fig 3. (A) HSPC support on OP9 stroma is not significantly affected by JAG1 blockade. Co-culture was performed as in Fig 3D using OP9 cells instead of hPSC-derived mesenchyme. Shown is CD34+Lin− cell number with addition of Goat IgG or human JAG1 blocking antibody to hPSC-mesenchyme co-culture (mean and SEM shown, n=4 independent experiments). **(B)** Neither over-expression nor inhibition of the WNT inhibitor SFRP1 in hPSC-mesenchyme co-cultures had a significant effect on HSPC *ex vivo* maintenance. Co-culture of CB-derived CD34+ with hPSC-derived $CD146^{hi}CD73^{hi}$ and $CD146^{lo}CD73^{lo}$ mesenchymal cells was performed as described previously. Shown is number of CD34+Lin− cells after addition of soluble SFRP1 or SFPR1 inhibitor (see supplemental methods) (mean and SEM are shown, n=3 independent experiments).

Table S1. Highly regulated genes shared by primary/hPSC derived cells. Related to Fig 4. (see excel file Table S1) Gene set enrichment analysis (GSEA) identifies a core set of genes differentially regulated between CD146+ vs. CD146- cells. A gene signature was defined from RNA-Seq of hPSC-derived mesenchymal cells (at least 2-fold up-, down-regulated between $CD146^{hi}CD73^{hi}$ vs. $CD146^{lo}CD73^{lo}$ cells, FDR<10%). The gene signature was compared to RNA-Seq fold changes from lipoaspirate-derived CD146+ and CD146- cells. GSEA was used to identify genes similarly regulated between hPSC-derived and A) freshly purified AND/OR B) cultured lipoaspirate-derived cells. Genes in the table represent the intersection between A) AND B).

SUPPLEMENTAL EXPERIMENTAL PROCEDURES

hESC culture and mesoderm induction conditions

The hESC lines H1 (WiCell, Madison, WI), UCLA3 and UCLA6 (UCLA BSCRC hESC core) were maintained and expanded on irradiated primary mouse embryonic fibroblasts (EMD Millipore, Billerica, MA). To induce mesoderm differentiation, hESC colonies were cut into uniform-sized pieces using the StemProEZPassage tool (Invitrogen, Thermo Fisher Scientific, Waltham, MA), transferred into 6-well plates pre-coated for 1 hour with Matrigel (growth factor reduced, no phenol red; BD Biosciences, San Jose, CA), and cultured initially in mTESR medium (Stem Cell Technologies, Vancouver, BC) until 50–60% confluent (typically 3 days). To initiate mesoderm differentiation, mTESR medium was replaced with basal induction medium X-Vivo 15 (Lonza, Walkersville, MD). Basal induction medium was supplemented with human growth factors BMP4, VEGF and bFGF for 3.5 days (all at 10 ng/mL; R&D Systems, Minneapolis, MN), with the inclusion of activin A only on day 1 ("A-BVF" condition (Evseenko et al., 2010)). After 3.5 days of mesoderm induction, $CD326^{-}CD56^{+}$ human embryonic mesoderm progenitors (hEMP) were isolated by flow cytometry (typically 5-10% of total population, **Figure 1A**) and placed onto matrigel coated 6 well plates for mesenchymal differentiation over the next 14-18 days.

Flow cytometry and cell sorting

Flow cytometry analysis was performed on LSRII or LSRFortessa and cell isolation on a FACSAria II (all from Becton Dickinson). Cultured cells were dissociated into single cell suspension with Accutase (Innovative Cell Technologies, San Diego, CA) and immunofluorescence staining was performed with human-specific monoclonal antibodies. Nonspecific binding was blocked with intravenous immunoglobulin (1%) (CSL Behring, King of Prussia, PA) before staining with fluorochrome-conjugated antibodies. Unstained cells and fluorescence-minus-one (FMO) were used as controls for gating. Cell acquisition was performed using FACSDiva (Becton Dickinson) and the analysis was performed using FlowJo (Tree Star, Ashland, OR). Forward and side scatter (FSC/SSC) and 4',6-diamidino-2-phenylindole (DAPI) (Invitrogen) were used to identify live cells.

Immunophenotype analysis of hEMP-derived mesenchyme

hEMP-derived mesenchyme at d14-18 of differentiation were harvested and analyzed on an LSR II flow cytometer (Becton Dickinson). Cells were stained with monoclonal antibodies: CD146-FITC (AbD Serotec, MCA2141FT) (for isolation) or CD146-BV711 (BD Biosciences, 563186) (for analysis), CD73-PE Cy7 (BD Biosciences, 561258), CD45-BV711 (Biolegend, 304050), CD31-APC (Biolegend, 303116), CD144-PE (BD Biosciences, 560410), CD34-PE Cy7 (BD Biosciences, 348791), CD105-PE (Biolegend, 323206), CD90-PE (Biolegend, 328110), CD44-PE (Biolegend, 338808), CD140a-PE (BD Biosciences, 556002), CD140b-PE (Biolegend, 323606), CSPG4-PE (BD Biosciences, 562415). Unstained cells and fluorescence-minus-one (FMO) were used as controls for gating.

To isolate the mesenchymal population by flow cytometry, the following gating sequence was used: CD31-APC (Biolegend, 303116) identified the endothelial population. From the non-endothelial compartment ($CD31^{-}$), the mesenchymal populations were identified based on CD73-PE-Cy7 (BD Biosciences, 561258) expression (i.e. $CD31^{-}CD73^{+}$). The CD146-FITC (AbD Serotec, MCA2141FT) bright cells were gated as $CD146^{hi}CD73^{hi}$ mesenchyme, and CD146-FITC negative cells were gated as $CD146^{lo}CD73^{lo}$ mesenchyme.

Flow cytometric analysis of cultured CB $CD34^{+}$ cells

After 2 weeks of co-culture, cells were harvested and stained with the following antibodies: CD45-BV711 (Biolegend, 304050), CD34-APC Cy7 (Biolegend, 343514), CD14-BV605 (Biolegend, 301834), CD10-PE Cy7 (Biolegend, 312214), CD33-PE (BD Biosciences, 347787), CD19-BV510 (Biolegend, 302242), FITC anti-human Lineage Cocktail (CD3, CD14, CD16, CD19, CD20, CD56) (Biolegend, 348801), CD90-APC (Biolegend, 328114), CD45RA-PerCP-Cy5.5 (Biolegend, 304122).

Colony forming unit assay

After 2 weeks of co-culture on mesenchymal monolayers, cells were harvested and plated in methylcellulose (Methocult 4434; Stem Cell Technologies) at 2.5×10^3 cells/well. Colonies were scored after 14 days and reported as the sum of the progeny of colony forming unit (CFU) granulocyte-macrophage (CFU-GM), burst-forming unit erythroid (BFU-E), and CFU mixed/CFU GEMM .

In vivo repopulation assay

CB CD34^{+} cells were co-cultured with CD146^{hi}CD73^{hi} or CD146^{lo}CD73^{lo} monolayers for 2 weeks. After flow cytometry analysis, an equal number of CD45^{+} cells (1 x 10^{5}) was obtained from the co-cultures and was intratibially injected into each sublethally irradiated (250 cGy), 6- to 8-week-old NSG mouse (The Jackson Laboratory). Control animals received 1 x 10^{5} non-cultured CD45+ cells from the same CB. Mice were sacrificed 6 weeks post-transplantation. Engraftment of human hematopoietic cells was evaluated by FACS analysis after staining with anti-human specific monoclonal antibodies: CD45-APC Cy7, HLA (A/B/C)-PE, CD34-PE Cy7, CD14-APC, CD19-FITC (all from BD Biosciences, 557833, 555553,348791, 340436, 555412). Engraftment was defined as presence of huCD45+HLA+ cells in at least 1 % of the bone marrow. For secondary transplantation, bone marrow from left and right tibias and femurs from each engrafted mouse was pooled and intra-tibially injected into a secondary host (one to one transplant). Engraftment was evaluated 6 weeks after secondary transplantation (12 weeks total). All animal studies were performed under a protocol approved by the UCLA animal care and use committee.

Transwell Experiments
Co-cultures were performed in HTS Transwell 96 Permeable Support Culture Plate System, 0.4µm Polycarbonate Membrane (Corning). Contact= mesenchyme and CB CD34+ both plated on the bottom well. No Contact= mesenchyme plated on the bottom well, CB CD34+ cells plated on the top well.

Notch and Wnt experiments
For the inhibition of JAG1, 1 µg/ml of anti-Jag1 N-17 (sc-34473, Santa Cruz Biotechnology) was added to each well every 48 hours from d0 to time of analysis at d13. An equal concentration of irrelevant Goat IgG (Sigma I9140) was added to wells as negative controls for anti-Jagged1 antibody.

For analysis of effects of sFRP-1 and Wnt signaling, 2 µg/ml recombinant human sFRP-1 protein (R&D Systems), 10uM WAY 316606 hydrochloride (sFRP-1 inhibitor) (R&D Systems) or 3uM CHIR99021 ("CHIR"=CHIR99021, Wnt agonist, GSK3 inhibitor) (Tocris Bioscience) were added to each well every 48 hours from d0 to time of analysis at d14. An equal volume of dimethylsulfoxide (DMSO; Sigma) was added to wells as negative control for WAY 316606 and CHIR99021 treatment.

Cell cycle analysis
At d14 of mesenchymal differentiation from hEMP, 1 mM BrdU (diluted in EGM-2 supplemented with SB-431542) was added to the culture for 40 minutes before harvesting cells for flow cytometry analysis. BrdU incorporation was measured using the FITC BrdU Flow Kit (BD Biosciences). The cell-cycle phases were defined as apoptotic (BrdU^{-} and DNA<2n), G0/G1 (BrdU^{-} and 2n DNA), S (BrdU+ and 2n≤DNA≤ 4n) and G2/M (BrdU^{-} and 4n DNA).

Quantitative RT-PCR
Freshly sorted hEMP-derived mesenchyme subsets (CD146^{hi}CD73^{hi} and CD146^{lo}CD73^{lo}) were processed for RNA extraction using a Qiagen micro kit. An Omniscript reverse transcriptase (RT) kit was used to make complementary DNA, which was subjected to quantitative polymerase chain reaction (qPCR) using Taqman probe-based gene expression assay (Applied Biosystems) and β2 microglobulin (β2M) as housekeeping gene. Best coverage primer/probe sets were selected for all target genes (*MCAM, IGFBP2, KITLG, LEPR, NES* and *CSPG4*). A 7500 real-time PCR system was used (ABI). Data were analyzed using the comparative ΔΔCT method.

For the Notch and Wnt target gene expression assays, co-culture of CB CD34+ cells with CD146^{hi}CD73^{hi} or CD146^{lo}CD73^{lo} was performed as described. 7 days after co-culture, cells were harvested and isolated as CD34+ cells and Lin+ cells by flow cytometry. RNA extraction and qPCR was performed as above to examine the expression of target genes *HES1*, *TCF7* and *LEF1*.

Taqman primers
For Quantitative RT-PCR, best coverage primer/probe sets were selected for all target genes as following:

	Assay ID
JAG1	Hs01070032_m1
HES1	Hs00172878_m1
TCF7	Hs01556515_m1

LEF1	Hs01547250_m1
MCAM	Hs00174838_m1
IGFBP2	Hs01040719_m1
KITLG	Hs00241497_m1
LEPR	Hs00174497_m1
NES	Hs04187831_g1
CSPG4	Hs00361541_g1
SFRP1	Hs00610060_m1
B2M	Hs00187842_m1

Isolation of human primary pericytes from lipoaspirate and RNA-Seq
Human pericytes were derived from human lipoaspirate specimens obtained as discarded anonymous waste tissue and thus deemed exempt from institutional review board approval. One hundred milliliters of lipoaspirate were incubated at 37°C for 30 minutes with digestion solution composed by RPMI-1640 (Cellgro), 3.5% bovine serum albumin (Sigma), and 1 mg/mL collagenase type II (Sigma). Adipocytes were discarded after centrifugation while the pellet was resuspended and incubated in red blood cell lysis (eBioscience) to obtain the stromal vascular fraction (SVF). SVF was processed for fluorescence-activated cell sorting (FACS).

Cells were incubated with the following antibodies: CD45-APC Cy7 (BD Biosciences), CD34-APC (BD Biosciences), and CD146-FITC (AbD Serotec). The viability dye 4,6 diamidino-2-phenylindole (DAPI; Sigma) was added before sorting on a FACS Aria III (BD Biosciences). $DAPI^{-}CD45^{-}CD34^{-}CD146^{+}$ were gated as pericytes and DAPI-CD31-CD45-CD34+CD146- were gated as adventitial cells.

For RNA-Seq, lipoaspirate-derived adventitial cells (CD31-CD45-CD34+CD146-) and pericytes (CD31-CD45-CD34-CD146+) were sorted from two donors. A fraction was pelleted for RNA extraction and the remaining cultured for 3 passages in DMEM containing 20% FBS. Following three passages in culture, the adventitial cells were pelleted for RNA extraction. Because of phenotype drifting, the pericytes were resorted for a consistent phenotype (CD31-CD45-CD34-CD146+) prior to collection for RNA extraction.

50ng of total RNA was extracted from a given population obtained from each of two donors and combined to yield a pooled sample of 100ng of total RNA. The samples were sequenced on an Illumina HiSeq 2000 using paired-end 100bp reads to a depth of coverage of ~ 10-15 million reads.

Isolation of human $CD34^{+}$ cells from CB
Umbilical cord blood (CB) was collected from normal deliveries without individually identifiable information, therefore no institutional review board approval was required. MNCs were isolated by density gradient centrifugation using Ficoll-Paque (GE Healthcare). Enrichment of $CD34^{+}$ cells was then performed using the magnetic-activated cell sorting system (Miltenyi Biotec) as per the manufacturer's instructions. Only samples with >80% purity were used in experiments.

RNA-Seq and analysis
hEMP ($CD326^{-}CD56^{+}$ cells) and freshly sorted day 14 hEMP-derived mesenchyme subsets ($CD146^{hi}CD73^{hi}$ and $CD146^{lo}CD73^{lo}$) were extracted with Trizol and purified using miRNeasy Mini Kit (Qiagen). Three biological replicates were obtained for each population. 500ng-2ug of total RNA was input to generate cDNA using Nugen Ovation RNA-Seq System v2 and the sequencing libraries were generated using prepX DNA library enzyme kit (IntegenX Inc.) per manufacturer's instructions. Paired-end 100bp sequencing was performed on Illumina HiSeq 2000 with six samples multiplexed per lane. Raw sequence files were obtained using Illumina's proprietary software and are available at NCBI's Gene Expression Omnibus (accession number GSE77879 and GSE83443).

RNA-Seq reads were aligned using STAR v2.3.0 (Dobin et al., 2013). The GRCh37 assembly (hg19) of the human genome and the corresponding junction database from Ensemble's gene annotation were used as reference for STAR. The count matrix for genes in the Ensembl genome annotation was generated with HTSeq-count v0.6.1p2 (Anders et al., 2015). DESeq v1.14.0 (Anders and Huber, 2010) was used for normalization (using the geometric mean across

samples), differential expression (to classify genes as differentially expressed, Benjamini-Hochberg adjusted p-value < 0.01) and to compute moderate expression estimates by means of variance-stabilized data. Heatmaps were built with GENE-E (http://www.broadinstitute.org/cancer/software/GENE-E/) applying relative min/max normalization to moderate expression estimates. Gene expression estimates of hPSC (H1 line), hEMP, hPSC-derived mesenchyme and lipoaspirate-derived mesenchyme were available in Table S1.

Gene Set Enrichment Analysis and STRING protein interaction analysis

Gene Set Enrichment Analysis (GSEA) (Subramanian et al., 2005) was used to perform the comparative analysis between the RNA-Seq expression signatures of hEMP-derived and lipoaspirate pericytes. The differentially expressed genes in hPSC-derived $CD146^{hi}CD73^{hi}$ vs $CD146^{lo}CD73^{lo}$ mesenchyme (fold change>2, FDR<0.01) defined the gene set of interest (*positive signature*: upregulated genes (n=540); *negative signature*: downregulated genes (n=351)). In both cases, the background for enrichment consisted of a ranked gene list where top ranking genes were more expressed in lipoaspirate-derived CD146+ pericytes as compared to CD146- cells. GSEA was run independently using both freshly sorted and cultured cells as background. For the positive (negative) signature, significant enrichment was only found for genes up- (down-) regulated in both freshly sorted and cultured lipoaspirate-derived CD146+ pericytes. The core gene sets provided by GSEA (highlighted in grey in Fig 4A, B) were further filtered for those genes that are consistently up or downregulated in $CD146^{++}$ from all sources. This final $CD146^{++}$ gene expression signature was then imported into the STRING database (Jensen et al., 2009). For protein interaction analyses, STRING (version 10) was used with default parameters. GO enrichment analysis was performed to identify the biological processes involved in the predicted STRING protein network.

SUPPLEMENTAL REFERENCES

Anders, S., and Huber, W. (2010). Differential expression analysis for sequence count data. Genome Biol *11*, R106.

Anders, S., Pyl, P.T., and Huber, W. (2015). HTSeq-a Python framework to work with high-throughput sequencing data. Bioinformatics *31*, 166-169.

Dobin, A., Davis, C.A., Schlesinger, F., Drenkow, J., Zaleski, C., Jha, S., Batut, P., Chaisson, M., and Gingeras, T.R. (2013). STAR: ultrafast universal RNA-seq aligner. Bioinformatics *29*, 15-21.

Evseenko, D., Zhu, Y., Schenke-Layland, K., Kuo, J., Latour, B., Ge, S., Scholes, J., Dravid, G., Li, X., MacLellan, W.*, et al.* (2010). Mapping the first stages of mesoderm commitment during differentiation of human embryonic stem cells. Proceedings of the National Academy of Sciences of the United States of America *107*, 13742-13747.

Jensen, L.J., Kuhn, M., Stark, M., Chaffron, S., Creevey, C., Muller, J., Doerks, T., Julien, P., Roth, A., Simonovic, M.*, et al.* (2009). STRING 8--a global view on proteins and their functional interactions in 630 organisms. Nucleic Acids Res *37*, D412-416.

Subramanian, A., Tamayo, P., Mootha, V.K., Mukherjee, S., Ebert, B.L., Gillette, M.A., Paulovich, A., Pomeroy, S.L., Golub, T.R., Lander, E.S.*, et al.* (2005). Gene set enrichment analysis: a knowledge-based approach for interpreting genome-wide expression profiles. Proc Natl Acad Sci U S A *102*, 15545-15550.